FEBS Letters 580 (2006) 849–861

Cholesterol loading augments oxidative stress in macrophages

Yao-Ching Hung[a], Meng-Yen Hong[b], G. Steve Huang[b,*]

[a] Section of Gynecologic Oncology, Department of Obstetrics and Gynecology, China Medical University and Hospital, Taiwan
[b] Institute of Nanotechnology, National Chiao Tung University, 1001 University Road, E5A02, Hsinchu 300, Taiwan

Received 5 October 2005; revised 30 December 2005; accepted 30 December 2005

Available online 18 January 2006

Edited by Laszlo Nagy

Abstract To investigate the molecular consequence of loading free cholesterol into macrophages, we conducted a large-scale gene expression study to analyze acetylated-LDL-laden foam cells (AFC) and oxidized-LDL-laden foam cells (OFC) induced from human THP-1 cell lines. Cluster analysis was performed using 9600-gene microarray datasets from time course experiment. AFC and OFC shared common expression profiles; however, there were sufficient differences between these two treatments that AFC and OFC appealed as two separate entities. We identified 80 commonly upregulated genes and 48 commonly downregulated genes in AFC and OFC. Functional annotation of the differentially expressed genes indicated that apoptosis, extracellular matrix, oxidative stress, and cell proliferation was deregulated. We also identified 87 differentially expressed genes unique for AFC and 31 genes for OFC. The uniquely expressed genes of AFC are associated with kinase activity, ATP binding activity, and transporter activity, while unique genes for OFC are associated with cell signaling and adhesion. To validate the hypothesis that oxidative stress is a common feature for AFC and OFC, we performed a cluster analysis employing the genes related to oxidative stress, but we were unable to distinguish AFC from OFC in this manner. We performed real-time RT-PCR and ELISA on foam cells to examine the transcripts and secreted protein of interleukin 1 beta (IL1β). IL1β was rapidly induced in foam cells, but for AFC both RNA level and protein level dropped immediately and was attenuated. To detect levels of reactive oxygen species in foam cells we conducted hydroethidine staining and observed high levels of superoxide anion. We conclude that loading free cholesterol induces high levels of superoxide anion, increases oxidative stress, and triggers a transient inflammatory response in macrophages.
© 2006 Published by Elsevier B.V. on behalf of the Federation of European Biochemical Societies.

Keywords: Low-density lipoproteins; Foam cells; Microarray; Atherosclerosis; Macrophages; Oxidized LDL; Acetylated LDL; Apoptosis; Expression pattern; Inflammatory response; Real-time RT-PCR

1. Introduction

The pathogenesis of cardiovascular disease, which is the leading cause of death in developed countries, occurs initially through atherosclerosis [1,2]. High levels of low-density lipoproteins (LDL) and oxidative stress are primary risk factors for the development of atherosclerosis [3–6]. Foam cells, which are the hallmark of an early atherosclerotic lesion, form as a result of a macrophage internalizing oxidized LDL (ox-LDL) through a scavenger receptor without feedback control [7–10]. These foam cells initiate an increase in oxidative stress and stimulate proliferation of smooth muscle cells in vitro [11–16].

The genetic consequences of macrophages taking up ox-LDL have been investigated broadly. Ox-LDL induces pro-inflammatory genes, activates PPARγ, and influences the expression of downstream genes. The induced macrophages secrete interleukin-1 beta (IL1β), which is a potent growth factor for smooth muscle cells (SMCs) [17]. IL1β may stimulate the SMCs to over-express platelet-derived growth factor (PDGF), which may cause migration and proliferation of the SMCs. Ox-LDL is toxic to macrophages; it causes the apoptosis and necrosis of foam cells and the subsequent release of their cellular contents, which may compose the necrotic core found in advanced lesions [18–21]. Large-scale surveys of the gene expression in ox-LDL-loaded foam cells have been performed on genome-wide scale [22–31]. Molecular markers are implicated in the cell growth, survival, migratory, inflammatory, and matrix remodeling of macrophages.

Oxidative modification transforms LDL into a powerful pathogen, but it is not clear whether the oxidative stress of foam cells is due to the oxidative modification of ox-LDL or to the cellular processing that follows the internalization through binding to the scavenger receptor. Acetylated LDL (ac-LDL), a non-oxidatively modified LDL, is readily taken up by macrophages, through a scavenger receptor, to generate foam cells [32–36]. Ac-LDL induces apoptosis and also inflammatory response in macrophages [37]. It is likely, but yet to be proven, that the internalized free cholesterol, analogous to oxidized LDL, triggers cellular pathways that lead to the increase in oxidative stress.

To evaluate the contribution of internalized cholesterol to the atherosclerotic behavior of foam cells, we conducted large-scale expression profiling of foam cells derived from both ox-LDL and ac-LDL [38]. Our results provide insights into the molecular mechanisms that distinguish the intracellular and extracellular oxidative events.

2. Materials and methods

DMEM, FBS, antibiotics, and all other tissue culture reagents were obtained from GIBCO. $CuSO_4$, KBr, thiobarbituric acid, trichloroacetic acid, and other common chemicals were purchased from Sigma or Merck.

2.1. Isolation of LDL and copper-mediated oxidation of LDL

LDL, in the density range 1.019–1.063, was isolated from human plasma through ultracentrifugation as described [39]; the typical protein concentration was 5 mg/ml. Copper-mediated oxidation was performed, as described in Mao et al. [40], through the addition of

*Corresponding author. Fax: +886 3 5753956.
E-mail address: gstevehuang@mail.nctu.edu.tw (G.S. Huang).

0014-5793/$32.00 © 2006 Published by Elsevier B.V. on behalf of the Federation of European Biochemical Societies.
doi:10.1016/j.febslet.2005.12.102

various concentrations of $CuSO_4$ into LDL and subsequent incubation at 37 °C for 16 h. The reaction was terminated upon the addition of excess EDTA.

2.2. Human macrophage cell lines THP-1

Human THP-1 cells were added to six-well tissue culture plates containing glass cover slips at 2×10^6 cells/well in DMEM containing 10% fetal bovine serum and 100 μg/ml penicillin; they were cultured for 4 h at 37 °C in an incubator containing 5% CO_2 at 90% humidity. The non-adherent cells were removed and the monolayers were then placed in DMEM containing 10% fetal bovine serum and supplemented with 100 μg/ml ox-LDL or ac-LDL. Foam cell formation was monitored by Oil Red O staining [41]. Monolayers of macrophages on glass cover slips were fixed with 10% formaldehyde in PBS (pH 7.4) for 10 min at room temperature, stained with Oil Red O, counterstained for 10 min with hematoxylin, and then examined under a microscope.

2.3. Microarray analysis

Inconsistent handling of microarray experiments frequently generates data that is difficult to process, especially for the time course experiment. We carefully initiated all experiments at the same starting point. Once a sample was harvested, we proceeded to cDNA synthesis and stored the labeled cDNA at −80 °C until use. All microarray hybridizations were conducted at the same time.

All microarray procedures – including PCR amplification, spotting, post-spotting processing, RNA extraction, probe preparation, hybridization, and post-hybridization experiments – were performed in a dust/climate controlled laboratory. Microarray design, experimental procedures, data processing, and data presentation were carefully performed according to the MIAME guidelines [42]. A microarray consisting of 9600 sequence-verified human cDNA was utilized in this current study [43].

The microarray experiment for each time point was performed in duplicate. Total RNA was extracted using the protocol supplied with the TRI reagent (Molecular Research Center, Inc., USA). The quality of the RNA was examined through agarose gel electrophoresis; the OD 260/280 ratio was >1.8. In a typical labeling reaction, total RNA (0.5–10 μg) was annealed with polydT(15) (0.5 μg) in a total volume of 20 μL. The cDNA synthesis was performed in 1× Superscript RT II reaction buffer (50 μL) containing annealed RNA, 0.5 mM each of dATP, dGTP, and dTTP, 40 μM of dCTP and Cy3-dCTP or Cy-5-dCTP (Roche, USA), 10 mM DTT, 1 U of RNasin (Invitrogen, USA), and 50 U of Superscript RT II (Invitrogen). The mixture was incubated in the dark for 90 min at 42 °C and the reaction was terminated through heating at 95 °C for 5 min. The RNA was degraded through the addition of 3 N NaOH (5.5 μL) and incubation at 50 °C for 30 min. The mixture was neutralized upon the addition of 3 M acetic acid (5.5 μL) and filter-purified through a Microcon YM-100 (Amicon Co., USA) to a final volume of 30 μL. Using a 50-mL conical tube, the microarray was prehybridized at 42 °C for 1 h in a prehybridization buffer (30 ml) containing 25% formamide, 5× SSC, 0.1% SDS, and 0.1 mg/mL BSA. The labeled probe was mixed with polydA(10) (20 μg) and human Cot-1 DNA (20 μg; Invitrogen) and then denatured at 95 °C for 5 min. The denatured probe was dried and suspended in the prehybridization buffer (20 μL). Hybridization was performed in a Corning hybridization chamber and incubated at 42 °C for 12–16 h. The slide was washed twice with 2× SSC and 0.1% SDS (30 ml) for 5 min at room temperature, followed by three washes (30 ml each; 20 min each) with 0.1× SSC and 0.1% SDS at 42 °C. All washing procedures were performed through gentle shaking in 50-mL conical tubes. Fluorescence scanning was performed using an Axon Genepix 4000B. The fluorescent image was processed by GenePix Pro 3.0 to obtain the raw expression dataset. The mean intensity and mean background intensity were utilized for data processing; the global array intensity was employed for normalization controls. Non-linear normalization was performed using locally weighted linear regression (lowess) [44]. Logarithmic ratios (base 2) were calculated accordingly. Duplicated data were averaged to obtain single dataset for each time point.

2.4. Statistical analysis for microarray datasets

Differentially expressed genes of microarray datasets were derived firstly by significance analysis of microarrays (SAM) [45]. The *P*-values corresponding to each gene were obtained by a standard *t*-test. The multiplicity of *P*-values due to the consequence of performing statistical tests on many genes in parallel was resolved by SAM method. SAM assigns a score to each gene based on change in gene expression relative to standard deviation of measurements. SAM performs permutation for repetitive measurement to estimate false discovery rate (FDR). In the current study, we adjusted the gene expression threshold that gave mean number of false discovery to less than one gene. Additionally, significantly expressed genes derived from SAM were further filtered by the criterion set by twice of the standard deviation calculated from the averaged dataset.

2.5. Real-time reverse transcription polymerase chain reaction (RT^2 PCR)

Real-time PCR analysis was performed, according to the manufacturer's instructions, using an iQ™ SYBR green supermix (Bio-Rad, USA) and the specific primer pairs for selected genes and the primer pairs for ribosomal protein L18 as the reference gene. The threshold cycle number (C_t) was measured using the iCycler and its associated software (Bio-Rad; [46]). Relative transcript quantities were calculated using the $\Delta\Delta C_t$ method with ribosomal protein L18 as the reference gene amplified from the samples. ΔC_t is the difference in the threshold cycles of the sample mRNAs relative to those of the ribosomal protein L18 mRNA. $\Delta\Delta C_t$ is the difference between the values of ΔC_t of the THP-1 cell control and the foam cells. Values for fold-induction were calculated as $2^{\Delta\Delta C_t}$. RT^2PCR was performed in triplicate for each time point.

2.6. Hydroethidine staining

Hydroethidine is one of the best reagents currently available for measuring the intracellular concentration of the superoxide anion ($O2^{\cdot -}$) [47,48]. The superoxide anion reacts with hydroethidine to produce ethidium bromide, which binds to nuclear DNA and emits fluorescence. Cells were washed briefly with PBS, incubated with 5 μM hydroethidine for 30 min, and then washed with PBS to remove any excess dye prior to imaging. Fluorescence was detected using a laser scanning confocal microscope operated at excitation and emission wavelengths of 488 and 610 nm, respectively, and using a 585-nm long-pass filter. The optical density of the ethidium ion was normalized to the number of THP-1 cells and is expressed as the percentage maximal intensity of ox-LDL-derived foam cells.

2.7. Enzyme-linked immunosorbent assay (ELISA)

The secretion of IL1β protein upon stimulation of modified LDL was characterized by ELISA using anti-IL1β IgG. Culture media were measured for IL1β protein content. The acquired reading in optical absorbance unit was normalized by the maximum signal.

2.8. Statistical analysis

All data from RT^2PCR, ELISA, and hydroethidine staining are presented as means ± standard error of the mean (S.E.M.). Data sets were evaluated using one-way analysis of variance (ANOVA). The minimum level of significance was set at $P < 0.05$.

3. Results and discussion

To obtain large-scale gene expression patterns for lipid loaded macrophages, we conducted microarray experiments using cDNA microarray containing 9600 genes of sequence-verified human cDNA. We performed time-course experiments on both ac-LDL-laden foam cells (AFC) and copper-oxidized-LDL-laden foam cells (OFC) while using untreated THP-1 cell lines as the normal control. We harvested the cells 12, 24, 36, 48, and 72 h in duplicates after administration of the modified LDL. Total RNA was fluorescence-labeled and hybridized to the microarray; we then detected the intensities using a laser-excited scanner. After background subtraction, we performed non-linear normalization using lowess procedure [44]. We derived the final expression ratios by comparing the results to those of the untreated cell line; we transformed and the ratios to the $\log_2$ scale for further data processing.

Hierarchical clustering analysis was performed to identify gene clusters specific for AFC or OFC (Fig. 1). All microarray datasets were clustered based on the variation of expression ratios of 9600 genes. Genes were clustered based on similarity in their expression patterns among different time points. AFC and OFC appealed as two distinct entities in the dendrogram, indicating that AFC and OFC can be separated by the transcriptional pattern. Commonly up or downregulated gene clusters were in greater proportion and spotted instantly. Judging from the similar trends for the up and downregulated genes in both entities, the difference in the expression pattern was minimal. We could, however, identify two gene clusters that displayed distinct expression patterns (Fig. 1, gene clusters A and B).

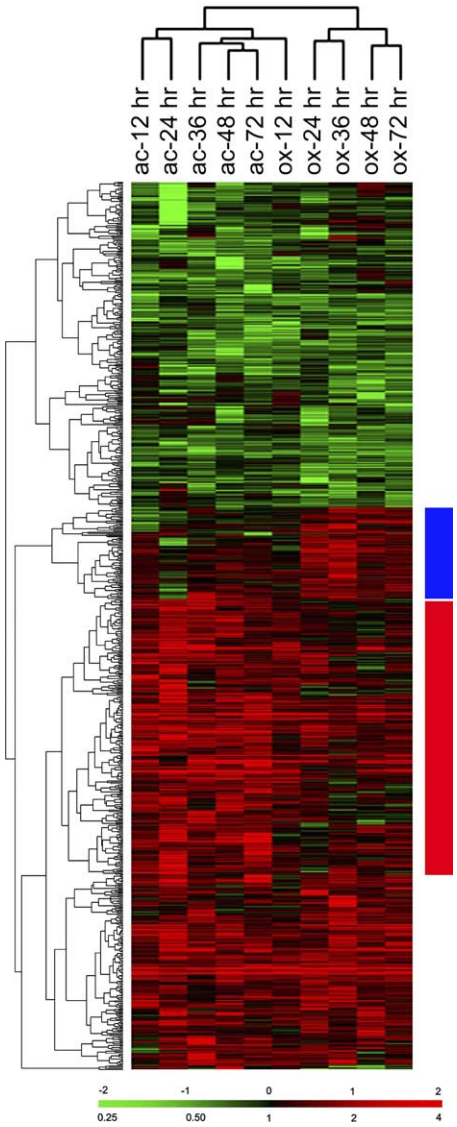

Fig. 1. Comparison of acetylated-LDL-loaded foam cells and oxidized-LDL-loaded foam cells using the gene expression ratios derived from the cDNA microarray. The diagram illustrates the results of hierarchical cluster analysis, which were visualized using Treeview software. Modified LDL was added to THP-1 cells, which were harvested after 12, 24, 36, 48, and 72 h. The foam cells are clustered based on the variation of the expression ratios of differentially expressed genes, which are themselves based on the criteria described in the text. Genes are clustered based on the similarities in their expression patterns among foam cells. Each column represents a specific treatment and each row a single gene. The colors, which reflect the ratios on the $\log_2$-based scale, are depicted in the scale bar at the bottom of the scheme. Green and red colors reflect lower- and higher-than-control levels of gene expression, respectively. The gene clusters that specify AFC-specific expression are highlighted with colored bars (blue, gene cluster A; red, gene cluster B).

Oxidized LDL utilizes a wide spectrum of scavenger receptors to enter macrophages; ac-LDL shares limited receptors encoded by SR-AI/II. In addition, the chemical modification of ac-LDL is non-oxidative. Thus the striking similarity in expression profiles between AFC and OFC implied that lipid deposition might contribute in major part the pathogenic transition from macrophages to foam cells. However, functional annotation to gene clusters common or unique to each type of foam cells might provide further insights to the molecular mechanisms that lead to atherogenesis.

3.1. *Differentially expressed genes common to ac-LDL- and ox-LDL-laden foam cells*

Based on a previous report, a significant molecular response can be observed before our first harvest time point [28]. For the purpose of obtaining differentially expressed genes, the individual time points in the time course experiments should be treated equally. In the current study, we applied two methods to identify the genes differentially expressed in AFC and OFC: the SAM method to select the overall differentially expressed genes [45] and the standard deviation (S.D.) to provide the threshold. The multiplicity of *P*-values due to the consequence of performing statistical tests on many genes in parallel was resolved by SAM method. We applied the SAM analysis to identify 323 upregulated genes and 124 downregulated genes from the overall datasets; the values of the median number of false positives, the false discovery rate, and delta were 0.56%, 0.13%, and 0.897%, respectively. As a screening filter we also applied the standard deviation of the microarray datasets of both the AFC and OFC samples; candidate genes having folds higher or lower than twice the SD were selected. We identified 315 upregulated genes and 165 downregulated genes for AFC and 255 upregulated genes and 176 downregulated genes for OFC. Eighty of the upregulated genes and 48 of the downregulated genes (Table 1) satisfied all of the criteria (SAM, SD of AFC, and SD of OFC). The original microarray datasets – differentially expressed genes identified by SAM and by SD-filtering – have been posted on our website as supplementary material (140.113.133.133/download/foam cells; Tables 1–4, Supplementary Material).

The differentially expressed genes shared by both AFC and OFC exhibited abnormality in apoptosis, extracellular matrix, oxidative stress, and cell proliferation. A group of genes typical for cell death and proliferation was spotted. Of most interest are interleukin 1 beta (IL1β), v-akt murine thymoma viral oncogene homolog 1, epithelial membrane protein 1, epithelial membrane protein 3, sterile alpha motif and leucine zipper containing kinase AZK, cell division cycle 2, and cell division cycle 23. IL1β, which is an important mediator of the inflammatory response, is involved in a variety of cellular activities, including cell proliferation, differentiation, and apoptosis. IL1β polymorphism is the risk factor of myocardial infarction and ischemic stroke at a young age [49]. The upregulation of IL1β strongly suggests the induction of inflammatory response by internalized lipids.

AKT1 encodes a serine/threonine protein kinase. In the developing nervous system, AKT is a critical mediator of

Table 1
Commonly up or downregulated genes in foam cells

LLID[a]	Name	Symbol	AFC[b]	OFC	FC	*P*-value[c]	Pathway[d]
207	v-akt murine thymoma viral oncogene homolog 1	AKT1	0.52	0.53	0.52	0.00173	Regulation of cell cycle
208	v-akt murine thymoma viral oncogene homolog 2	AKT2	0.55	0.5	0.53	0	Regulation of cell cycle
229	Aldolase B, fructose-bisphosphate	ALDOB	0.53	0.55	0.54	0	Glycolysis
239	Arachidonate 12-lipoxygenase	ALOX12	0.42	0.47	0.44	0	Leukotriene biosynthesis
323	Amyloid beta (A4) precursor protein-binding, family B, member 2 (Fe65-like)	APBB2	2.6	1.8	2.3	0.00046	Cell cycle arrest
372	Archain 1	ARCN1	1.9	1.9	1.9	0.00006	Intracellular protein transport
720	Complement component 4A	C4A	0.5	0.41	0.46	0.00013	Inflammatory response
760	Ccarbonic anhydrase II	CA2	0.25	0.28	0.26	0	One-carbon compound metabolism
781	Calcium channel, voltage-dependent, alpha 2/delta subunit 1	CACNA2D1	3.1	2.4	2.8	0.00015	Ion transport
948	CD36 antigen (collagen type I receptor, thrombospondin receptor)	CD36	2.8	2.5	2.6	0	Fatty acid metabolism
983	Cell division cycle 2, G1 to S and G2 to M	CDC2	0.41	0.42	0.41	0.00098	Mitosis
987	LPS-responsive vesicle trafficking, beach and anchor containing	LRBA	6.6	3.9	5.3	0.00003	
1009	Cadherin 11, type 2, OB-cadherin (osteoblast)	CDH11	2	2.1	2	0.00013	Homophilic cell adhesion
1511	Cathepsin G	CTSG	0.39	0.39	0.39	0	Immune response
1511	Cathepsin G	CTSG	0.4	0.34	0.37	0.00028	Immune response
1519	Cathepsin O	CTSO	2.6	2.3	2.5	0	Proteolysis and peptidolysis
1535	Cytochrome *b*-245, alpha polypeptide	CYBA	0.42	0.39	0.41	0.00004	Superoxide metabolism
1536	Cytochrome *b*-245, beta polypeptide (chronic granulomatous disease)	CYBB	0.38	0.54	0.43	0.00005	Inflammatory response
1536	Cytochrome *b*-245, beta polypeptide (chronic granulomatous disease)	CYBB	0.37	0.54	0.43	0.00255	Inflammatory response
1565	Cytochrome P450, subfamily IID (debrisoquine, sparteine, etc., -metabolising), polypeptide 7a (pseudogene)	CYP2D7AP	2.6	2	2.3	0.00022	**Electron transport**
1741	Discs, large homolog 3 (neuroendocrine-dlg, Drosophila)	DLG3	2.6	2.2	2.5	0	**Negative regulation of cell proliferation**
1827	Down syndrome critical region gene 1	DSCR1	2.9	2.4	2.7	0.00005	Calcium-mediated signaling
1841	Deoxythymidylate kinase (thymidylate kinase)	DTYMK	0.51	0.45	0.48	0	DNA metabolism
1854	dUTP pyrophosphatase	DUT	0.45	0.46	0.45	0.00255	DNA replication
1893	Extracellular matrix protein 1	ECM1	0.54	0.44	0.5	0.00001	**Transport**
2012	Epithelial membrane protein 1	EMP1	3.2	3.7	3.4	0	Epidermal differentiation
2014	Epithelial membrane protein 3	EMP3	0.45	0.42	0.44	0.00001	Ccell growth
2335	Fibronectin 1	FN1	0.48	0.41	0.45	0.00093	Cell adhesion
3151	High-mobility group nucleosomal binding domain 2	HMGN2	2.4	2.4	2.4	0	Establishment and/or maintenance of chromatin architecture
3176	Histamine *N*-methyltransferase	HNMT	2.1	2.1	2.1	0	**Respiratory gaseous exchange**
3192	Heterogeneous nuclear ribonucleoprotein U (scaffold attachment factor A)	HNRPU	2.1	1.9	2	0.00011	**RNA processing**
3251	Hypoxanthine phosphoribosyltransferase 1 (Lesch-Nyhan syndrome)	HPRT1	2.5	2.4	2.5	0	Nucleoside metabolism
3553	Interleukin 1, beta	IL1β	2.2	2.3	2.2	0.00037	Inflammatory response
3566	Interleukin 4 receptor	IL4R	0.3	0.5	0.37	0.00209	Immune response
3601	Interleukin 15 receptor, alpha	IL15RA	0.53	0.53	0.53	0.00013	Cell proliferation
3866	Keratin 15	KRT15	2	1.8	1.9	0.00412	Epidermal differentiation
3934	Lipocalin 2 (oncogene 24p3)	LCN2	1.9	1.9	1.9	0.00002	Transport
4001	Lamin B1	LMNB1	0.48	0.41	0.45	0.00099	

4015	Lysyl oxidase	LOX	2.3	1.8	2.1	0.0004	**Protein modification**
4179	Membrane cofactor protein (CD46, trophoblast–lymphocyte cross-reactive antigen)	MCP	0.43	0.37	0.41	0	Invasive growth
4330	Meningioma (disrupted in balanced translocation) 1	MN1	2.7	1.8	2.3	0.00081	**Negative regulation of cell cycle**
4332	Myeloid cell nuclear differentiation antigen	MNDA	0.48	0.45	0.47	0.00004	Cellular defense response
4332	Myeloid cell nuclear differentiation antigen	MNDA	0.46	0.46	0.46	0.00003	Cellular defense response
4485	Macrophage stimulating 1 (hepatocyte growth factor-like)	MST1	4.1	2.2	3.2	0.00009	Proteolysis and peptidolysis
4613	v-myc myelocytomatosis viral related oncogene, neuroblastoma derived (avian)	MYCN	1.8	2.5	2.1	0.00003	Cell growth and/or maintenance
4649	Myosin IXA	MYO9A	2	2.3	2.1	0	Intracellular signaling cascade
4726	NADH dehydrogenase (ubiquinone) Fe–S protein 6, 13 kDa (NADH-coenzyme Q reductase)	NDUFS6	3.1	3.6	3.3	0	Mitochondrial electron transport, NADH to ubiquinone
4807	Nescient helix–loop–helix 1	NHLH1	3.1	2.6	2.9	0.00003	Cell differentiation
4907	5′-nucleotidase, ecto (CD73)	NT5E	3.8	4.6	4.1	0	DNA metabolism
4907	5′-nucleotidase, ecto (CD73)	NT5E	3.1	3.6	3.3	0.00005	DNA metabolism
5007	Oxysterol binding protein	OSBP	1.9	1.9	1.9	0.00252	Steroid metabolism
5125	Proprotein convertase subtilisin/kexin type 5	PCSK5	0.59	0.48	0.54	0.00024	Proteolysis and peptidolysis
5126	Proprotein convertase subtilisin/kexin type 2	PCSK2	2.2	2.4	2.3	0	Proteolysis and peptidolysis
5216	Profilin 1	PFN1	0.39	0.48	0.43	0.00323	**Actin cytoskeleton organization and biogenesis**
5229	Protein geranylgeranyltransferase type I, beta subunit	PGGT1B	1.8	2.3	2	0.00013	Protein amino acid geranylgeranylation
5230	Phosphoglycerate kinase 1	PGK1	2.7	1.9	2.3	0.00002	**Glycolysis**
5319	Phospholipase A2, group IB (pancreas)	PLA2G1B	1.9	1.8	1.9	0.00006	Lipid catabolism
5441	Polymerase (RNA) II (DNA directed) polypeptide L, 7.6 kDa	POLR2L	2.4	1.9	2.2	0.00022	Regulation of transcription from Pol I promoter
5465	Peroxisome proliferative activated receptor, alpha	PPARA	4.1	3.5	3.8	0	Regulation of fatty acid metabolism
5465	Peroxisome proliferative activated receptor, alpha	PPARA	2.6	2.6	2.6	0.00005	Regulation of fatty acid metabolism
5468	Peroxisome proliferative activated receptor, gamma	PPARG	5.1	2.9	4.1	0	Lipid metabolism
5636	Phosphoribosyl pyrophosphate synthetase-associated protein 2	PRPSAP2	0.46	0.5	0.48	0.00204	Nucleoside metabolism
5699	Proteasome (prosome, macropain) subunit, beta type, 10	PSMB10	0.51	0.52	0.52	0.00029	Humoral immune response
5770	Protein tyrosine phosphatase, non-receptor type 1	PTPN1	1.8	2.1	1.9	0.00042	Protein amino acid dephosphorylation
5781	Protein tyrosine phosphatase, non-receptor type 11 (Noonan syndrome 1)	PTPN11	2.8	2	2.5	0.0008	Protein amino acid dephosphorylation
5792	Protein tyrosine phosphatase, receptor type, F	PTPRF	2.1	2	2.1	0.00026	Cell adhesion
5816	Parvalbumin	PVALB	1.8	1.9	1.8	0.00004	**Muscle development**
5836	Phosphorylase, glycogen; liver (Hers disease, glycogen storage disease type VI)	PYGL	0.6	0.45	0.53	0.00011	**Glycogen metabolism**
5911	RAP2A, member of RAS oncogene family	RAP2A	1.8	2.2	2	0.00009	**Small GTPase mediated signal transduction**
5919	Retinoic acid receptor responder (tazarotene induced) 2	RARRES2	0.52	0.52	0.52	0.00006	**Retinoid metabolism**
6036	Ribonuclease, RNase A family, 2 (liver, eosinophil-derived neurotoxin)	RNASE2	0.42	0.37	0.4	0	Chemotaxis
6182	Mitochondrial ribosomal protein L12	MRPL12	2.2	1.9	2	0.00118	**Protein biosynthesis**
6302	Sarcoma amplified sequence	SAS	0.51	0.54	0.52	0.00006	**Positive regulation of cell proliferation**
6392	Succinate dehydrogenase complex, subunit D, integral membrane protein	SDHD	3	2.6	2.8	0.00002	Electron transport
6418	SET translocation (myeloid leukemia-associated)	SET	2.1	1.9	2	0.0001	Oncogenesis
6444	Sarcoglycan, delta (35 kDa dystrophin-associated glycoprotein)	SGCD	0.53	0.47	0.51	0.00179	**Muscle development**
6710	Spectrin, beta, erythrocytic (includes spherocytosis, clinical type I)	SPTB	0.63	0.26	0.44	0.00035	
6745	Signal sequence receptor, alpha (translocon-associated protein alpha)	SSR1	0.53	0.42	0.48	0	Positive regulation of cell proliferation

(*continued on next page*)

Table 1 (*continued*)

LLID[a]	Name	Symbol	AFC[b]	OFC	FC	*P*-value[c]	Pathway[d]
7021	Transcription factor AP-2 beta (activating enhancer binding protein 2 beta)	TFAP2B	2.7	2	2.4	0.0001	Regulation of transcription from Pol II promoter
7056	Thrombomodulin	THBD	2.5	3.1	2.7	0.00008	Blood coagulation
7057	Thrombospondin 1	THBS1	0.34	0.44	0.38	0.00001	Cell adhesion
7289	Tubby like protein 3	TULP3	2	1.8	1.9	0.00421	G-protein coupled receptor protein signaling pathway
7298	Thymidylate synthetase	TYMS	0.41	0.48	0.43	0	**dTMP biosynthesis**
7298	Thymidylate synthetase	TYMS	0.37	0.55	0.43	0.00002	**dTMP biosynthesis**
7337	Ubiquitin protein ligase E3A (human papilloma virus E6-associated protein, Angelman syndrome)	UBE3A	2.8	1.9	2.4	0.00052	Ubiquitin-dependent protein catabolism
7378	Uridine phosphorylase 1	UPP1	1.8	2.2	1.9	0.00115	**Nucleoside metabolism**
8204	Nuclear receptor interacting protein 1	NRIP1	2.1	1.8	2	0.00005	**Regulation of transcription, DNA-dependent**
8519	Interferon induced transmembrane protein 1 (9–27)	IFITM1	0.34	0.46	0.38	0.00003	Immune response
8697	CDC23 (cell division cycle 23, yeast, homolog)	CDC23	0.49	0.34	0.42	0.00201	Cytokinesis
8906	Adaptor-related protein complex 1, gamma 2 subunit	AP1G2	2.8	2.4	2.6	0.00001	Intracellular protein transport
9145	Synaptogyrin 1	SYNGR1	4.1	2.7	3.5	0.00003	**Transport**
9314	Kruppel-like factor 4 (gut)	KLF4	0.5	0.52	0.51	0.00147	Negative regulation of cell proliferation
9486	Carbohydrate sulfotransferase 10	CHST10	1.9	2.3	2	0.00096	**Cell adhesion**
9653	Heparan sulfate 2-*O*-sulfotransferase 1	HS2ST1	0.54	0.52	0.53	0.00006	**Protein amino acid sulfation**
9820	Cullin 7	CUL7	1.8	1.9	1.8	0.00076	
9969	Thyroid hormone receptor associated protein 1	THRAP1	1.8	2.2	2	0	Androgen receptor signaling pathway
10121	ARP1 actin-related protein 1 homolog A, centractin alpha (yeast)	ACTR1A	0.51	0.48	0.49	0.00074	**Vesicle-mediated transport**
10215	Oligodendrocyte lineage transcription factor 2	OLIG2	2.4	2.6	2.5	0	Cell growth and/or maintenance
10216	Proteoglycan 4, (megakaryocyte stimulating factor, articular superficial zone protein, camptodactyly, arthropathy, coxa vara, pericarditis syndrome)	PRG4	0.33	0.5	0.39	0.00089	**Cell proliferation**
10262	Splicing factor 3b, subunit 4, 49 kDa	SF3B4	7.3	4	5.7	0.00016	**Nuclear mRNA splicing, via spliceosome**
10959	Coated vesicle membrane protein	RNP24	2.3	2	2.1	0.00083	**Intracellular protein transport**
10969	EBNA1 binding protein 2	EBNA1BP2	3.1	2.7	3	0	G-protein coupled receptor protein signaling pathway
10981	RAB32, member RAS oncogene family	RAB32	0.47	0.5	0.48	0.00008	Protein transport
11273	ataxin 2 related protein	A2LP	3.2	3.5	3.3	0	
11344	PTK9L protein tyrosine kinase 9-like (A6-related protein)	PTK9L	1.7	2.3	1.9	0.00069	**Intracellular signaling cascade**
22795	Nidogen 2 (osteonidogen)	NID2	2	2.1	2	0.00001	**Cell–matrix adhesion**
23203	Peptidase (mitochondrial processing) alpha	PMPCA	3.7	3.3	3.5	0	**Proteolysis and peptidolysis**
23209	Megalencephalic leukoencephalopathy with subcortical cysts 1	MLC1	3.1	2	2.6	0.0002	**Transport**
23358	Ubiquitin specific protease 24	USP24	2	1.8	1.9	0	**Ubiquitin-dependent protein catabolism**
25911	Deleted in a mouse model of primary ciliary dyskinesia	DPCD	2.8	2.1	2.5	0.00003	
26275	3-Hydroxyisobutyryl-coenzyme A hydrolase	HIBCH	2.4	1.8	2.2	0.00002	**Metabolism**
27316	RNA binding motif protein, X-linked	RBMX	2.4	2.3	2.4	0.00328	Regulation of transcription, DNA-dependent
29974	apobec-1 complementation factor	ACF	3.5	2.3	2.9	0	**mRNA editing**
50486	Putative lymphocyte G0/G1 switch gene	G0S2	0.47	0.43	0.45	0.00025	**Regulation of cell cycle**
51776	Sterile alpha motif and leucine zipper containing kinase AZK	ZAK	0.57	0.57	0.57	0.00018	Cell death
55336	Heat shock transcription factor 4	HSF4	0.52	0.53	0.53	0.00007	
55567	Dynein, axonemal, heavy polypeptide 3	DNAH3	2.7	2.1	2.4	0.00015	**Microtubule-based movement**
64714	Protein disulfide isomerase	PDI	2.2	1.9	2.1	0.00017	Electron transport
80204	F-box protein 11	FBXO11	2.1	2.2	2.1	0	Ubiquitin-dependent protein catabolism

80829	Cell cycle progression 2 protein	CPR2	2.1	2.3	2.2	0	
84809	Hypothetical protein MGC12760	MGC12760	1.8	2	1.9	0.00007	**Regulation of transcription, DNA-dependent**
112398	egl nine homolog 2 (*C. elegans*)	EGLN2	2.7	1.9	2.3	0.00085	Response to hypoxia
116984	Centaurin, delta 1	CENTD1	1.9	1.8	1.9	0.00002	**Neuropeptide signaling pathway**
121260	Ancient conserved domain protein 4	LOC56939	0.56	0.3	0.44	0.00073	**Oligopeptide transport**
130814	Chromosome 2 open reading frame 22	C2orf22	5.3	1.9	3.5	0.0001	
131578	Leucine rich repeat containing 15	LRRC15	1.7	2.1	1.8	0.00025	
154881	Potassium channel tetramerisation domain containing 7	KCTD7	3.1	2.3	2.8	0	**Potassium ion transport**
200734	Sprouty-related, EVH1 domain containing 2	SPRED2	6.4	4.8	5.7	0[c]	

[a]LLID is the locus link identification number that identifies a specific gene in GenBank.
[b]Values represent averaged fold change. AFC, ac-LDL-loaded foam cells; OFC, ox-LDL-laden foam cells; FC, mean value of AFC and OFC.
[c]*P*-values are results from *t*-test for all fold changes of the specific gene. "0" depicts *P*-values less than 0.00001.
[d]Pathway is derived from GO-biological process. The plain text depicts representative pathway among several possible pathways. The bold text depicts unique pathway. The complete table is available on our website.

growth factor-induced neuronal survival. Survival factors can suppress apoptosis in a transcription-independent manner by activating this serine/threonine kinase, which then phosphorylates and inactivates components of the apoptotic machinery. Immunostaining and microarray evidence suggests that AKT1 is downregulated at recurrent carotid stenosis [50]. The downregulation of AKT1 suggests activation of apoptotic machinery and is consistent with the observation that both AFC and OFC underwent apoptosis.

Extracellular matrix remodeling of foam cells has been suggested to occur through the downregulation of fibronectin and spectrin. Spectrin is the major constituent protein of the erythrocyte cytoskeleton that forms a filamentous network on the cytoplasmic face of the membrane. The major function of spectrin is presumed to be that of establishing the cytoskeletal network that provides mechanical strength to the cell membrane.

The differential expression for oxidative stress is indicated by arachidonate 12-lipoxygenase, cytochrome *b*-245 alpha and beta, cytochrome P450 2D6, lysyl oxidase, NADH dehydrogenase, protein disulfide isomerase, and egl nine homolog 2. Of particular interest is EGL nine homolog 2 [EGLN2 or hypoxia-inducible factor (HIF)], a transcriptional regulator that plays a key role in hypoxia [51]. Over-expression of ENGLN2 has been identified in the myocardial microvessels and coronary artery of a hypercholesterolimic pig [52]. Further studies into the role of EGLN2 during atherogenesis should prove insightful. The upregulation of LPS-responsive vesicle trafficking (LRBA) indicated that the delicate balance of intracellular cholesterol trafficking was severely disturbed [53,54]. The upregulation of 5′-nucleotidase, ecto (CD73), is consistent with the elevation of enzyme activity for CD73 in the human atherosclerotic aorta [55,56]. Additionally, the over-expression of peroxisome proliferative activated receptors (PPARA, PPARD), thrombomodulin (THBD), CD36, and interleukin 1 beta (IL1β) are consistent with the results of a previous report [57–61]. In particular, significant over-expression of cytochrome P450 and acyl-Coenzyme A dehydrogenase indicate the increase in oxidative stress in both AFC and OFC.

3.2. Genes that distinguish AFC and OFC

To identify gene clusters that distinguish AFC from OFC, we started with the gene clusters A and B from Fig. 1 and overlapped with differentially expressed genes that are statistically significant from microarray datasets. We obtained 87 AFC-specific genes (Table 2) and 31 OFC-specific genes (Table 3).

AFC-specific genes exhibited changes in the metabolic pathways including kinase activity, ATP binding activity, and transporter activity. Fifteen genes are categorized as kinase activity including. Of most interest are PCTAIRE protein kinases 1 and 3. These genes belong to the cdc2/cdkx subfamily of the ser/thr family of protein kinases. They may play a role in signal transduction cascades in terminally differentiated cells. Eight genes are involved in transporter activity. There are a few channel proteins including chloride channels (CLCN6, CLIC2, SLC12A4), potassium channels (KCNF1, KCNJ4, SLC12A4), proteins associated with mitochondria ion transport (FRDA, UCP3), and peroxisome-associated enzyme (DDO).

OFC-specific genes exhibited completely different functions in cell signaling and adhesion. The protein encoded by JAG2 activates Notch and related receptors. The Notch signaling pathway is an intercellular signaling mechanism that is

Table 2
Genes specifically up or downregulated in AFC

LLID	Symbol	AFC[a]	OFC	FC	OFC/AFC	*P*-value[b]	Pathway[c]
156	ADRBK1	1.95	0.98	1.48	0.5	0.00155	Signal transduction
229	ALDOB	0.52	0.86	0.64	1.64	0.01333	Glycolysis
808	CALM3	2.09	1.22	1.68	0.58	0.00564	
1121	CHM	3.09	1.55	2.34	0.5	0.00073	Non-selective vesicle transport
1185	CLCN6	1.93	1.08	1.53	0.56	0.00135	Chloride transport
1193	CLIC2	2.88	1.28	2.09	0.45	0.00021	**Chloride transport**
1361	CPB2	0.53	1.04	0.69	1.97	0.00034	**Proteolysis and peptidolysis**
1611	DAP	2.09	1.14	1.64	0.54	0.00103	**Induction of apoptosis by extracellular signals**
1659	DHX8	2.43	1.1	1.77	0.45	0.00205	**Nuclear mRNA splicing, via spliceosome**
1760	DMPK	2.37	1.43	1.94	0.6	0.00396	Protein amino acid phosphorylation
2098	ESD	1.9	1.06	1.51	0.56	0.0002	
2140	EYA3	2.47	1.3	1.91	0.53	0.00085	Morphogenesis
2261	FGFR3	2.43	0.97	1.69	0.4	0.00388	MAPKKK cascade
2275	FHL3	2.51	1.31	1.94	0.52	0.00561	**Muscle development**
2335	FN1	2.56	1.42	2.03	0.56	0.00123	Cell adhesion
2395	FRDA	2.03	1.06	1.57	0.52	0.00067	Vesicle-mediated transport
2553	GABPB1	2.07	1.14	1.63	0.55	0.0001	**Regulation of transcription from Pol II promoter**
2589	GALNT1	2.4	1.41	1.94	0.59	0.01466	Heterophilic cell adhesion
2592	GALT	2.64	1.29	1.98	0.49	0.01065	**Galactose metabolism**
2687	GGTLA1	1.81	0.96	1.4	0.53	0.00318	Glutathione biosynthesis
2737	GLI3	2.18	1.02	1.61	0.47	0.00496	Morphogenesis
2739	GLO1	0.49	0.85	0.61	1.75	0.00118	**Carbohydrate metabolism**
2899	GRIK3	2.48	1.06	1.76	0.43	0.01348	Glutamate signaling pathway
2932	GSK3B	2.43	1.23	1.85	0.5	0.01081	Anti-apoptosis
2939	GSTA2	2.29	1.18	1.76	0.51	0.01667	Glutathione conjugation reaction
3276	HRMT1L2	2.08	1.02	1.56	0.49	0.00061	Protein amino acid methylation
3754	KCNF1	2.16	1.11	1.66	0.51	0.00453	**Potassium ion transport**
3761	KCNJ4	0.33	0.73	0.45	2.2	0.01765	**Potassium ion transport**
3953	HSOBRGRP	1.8	1.08	1.47	0.6	0.00176	Cell surface receptor linked signal transduction
4034	LRCH4	0.44	0.77	0.55	1.74	0.00172	**Neurogenesis**
4043	LRPAP1	1.71	0.78	1.25	0.46	0.00297	Vesicle-mediated transport
4052	LTBP1	2.46	0.94	1.68	0.38	0.00625	
4324	MMP15	2.22	0.88	1.53	0.39	0.00051	Proteolysis and peptidolysis
4363	ABCC1	1.92	1.06	1.51	0.55	0.00422	Protein amino acid phosphorylation
4486	MST1R	2.75	1.35	2.07	0.49	0.00018	Protein amino acid phosphorylation
4515	MTCP1	2.14	1.03	1.6	0.48	0.01469	Regulation of cell cycle
5076	PAX2	0.4	0.88	0.55	2.17	0.00597	Cell differentiation
5127	PCTK1	2.32	1.39	1.89	0.6	0.02153	Protein amino acid phosphorylation
5129	PCTK3	2.11	1.21	1.69	0.57	0.00001	Protein amino acid phosphorylation
5272	SERPINB9	2.82	1.46	2.17	0.52	0.00671	
5351	PLOD	2.23	0.72	1.42	0.32	0.00145	Epidermal differentiation
5393	EXOSC9	2.22	1.11	1.68	0.5	0.00406	Immune response
5583	PRKCH	2.24	1.37	1.84	0.61	0.00005	Protein amino acid phosphorylation
5790	PTPRCAP	2.16	1.19	1.71	0.55	0.00084	
5983	RFC3	2.43	1.48	1.99	0.61	0.00114	**DNA strand elongation**
6259	RYK	1.95	1.15	1.58	0.59	0.00124	Protein amino acid phosphorylation
6370	CCL25	2.9	1.52	2.24	0.53	0.00356	Inflammatory response
6560	SLC12A4	2.05	1.19	1.65	0.58	0.0002	Potassium ion transport
6573	SLC19A1	1.85	0.92	1.4	0.5	0.00259	**Folate transport**
6645	SNTB2	2.23	1.14	1.7	0.51	0.0051	
6654	SOS1	0.56	1.68	0.87	3	0.00425	**RAS protein signal transduction**
6789	STK4	1.7	0.91	1.32	0.53	0.00035	Protein amino acid phosphorylation
6881	TAF10	2.22	1.13	1.69	0.51	0.00005	Transport
6947	TCN1	2.32	0.84	1.54	0.36	0.00681	Vitamin B12 transport
7059	THBS3	1.93	1.13	1.55	0.58	0.01054	Cell–matrix adhesion
7153	TOP2A	0.54	0.92	0.67	1.71	0.0062	**DNA topological change**
7287	TULP1	0.38	0.99	0.56	2.57	0.01052	**Vision**
7352	UCP3	2.29	1.38	1.87	0.6	0.01524	Lipid metabolism
7803	PTP4A1	2.65	1.39	2.05	0.52	0.00546	Protein amino acid dephosphorylation
8021	NUP214	2.14	1.03	1.6	0.48	0.00307	Oncogenesis
8091	HMGA2	2.3	0.79	1.5	0.34	0.0019	Development
8528	DDO	0.52	0.93	0.66	1.77	0.00003	Electron transport
8663	EIF3S8	1.88	1.12	1.53	0.59	0.0122	**Regulation of translational initiation**
9061	PAPSS1	2.15	0.8	1.45	0.37	0.00252	Sulfate assimilation
9094	UNC119	2.17	1.18	1.7	0.54	0.0032	Synaptic transmission
9334	B4GALT5	0.55	1.12	0.73	2.03	0.01625	Sphingolipid biosynthesis
9462	RASAL2	2.61	0.92	1.72	0.35	0.0009	**Signal transduction**
9540	TP53I3	0.49	1.04	0.66	2.1	0.01713	
10146	G3BP	2.55	1.27	1.93	0.5	0.00037	RAS protein signal transduction
10899	JTB	2.14	1.08	1.63	0.51	0.002	**Oncogenesis**

Table 2 (*continued*)

LLID	Symbol	AFC[a]	OFC	FC	OFC/AFC	*P*-value[b]	Pathway[c]
10914	PAPOLA	2.45	1.17	1.82	0.48	0.00489	
23016	EXOSC7	2.21	1.05	1.64	0.48	0.00132	RNA catabolism
23034	SAMD4	2.08	0.91	1.49	0.44	0.00819	
23301	NACSIN	0.56	0.93	0.69	1.68	0.01276	**Ubiquitin cycle**
23509	POFUT1	0.42	0.86	0.56	2.06	0.00141	N-signaling pathway
23518	R3HDM	0.56	1.19	0.75	2.14	0.00401	
23769	FLRT1	1.92	1.04	1.51	0.54	0.00229	Lipid catabolism
27254	PIPPIN	0.56	0.93	0.68	1.67	0.0011	mRNA processing
27347	STK39	2.81	1.56	2.22	0.56	0.00507	Protein amino acid phosphorylation
55168	MRPS18A	3.6	1.5	2.53	0.42	0.00109	**Protein biosynthesis**
55544	RNPC1	3.02	1.04	1.97	0.35	0.00274	
56928	SPPL2B	0.5	0.82	0.61	1.64	0.01513	**Proteolysis and peptidolysis**
58525	WIZ	2.78	1.2	1.98	0.43	0.00524	**Regulation of transcription, DNA-dependent**
80347	COASY	2.45	1.25	1.87	0.51	0.00591	**Coenzyme A biosynthesis**
84958	SYTL1	0.46	0.87	0.59	1.91	0.00932	**Transport**
85006	PDXK	2.18	1.18	1.71	0.54	0.00869	
124583	ENTPD8	1.87	1.13	1.53	0.6	0.00409	

[a]Values represent averaged fold change for all time course experiments. AFC, ac-LDL-loaded foam cells; OFC, ox-LDL-laden foam cells; FC, mean value of AFC and OFC. OFC/AFC depicts expression ratio of OFC compared to AFC.
[b]*P*-values are results from *t*-test for all fold changes of AFC.
[c]Pathway is derived from GO-biological process. The plain text depicts representative pathway among several possible pathways. The bold text depicts unique pathway. The complete table is available on our website.

essential for proper embryonic development and various cell fate decisions. Adhesion molecules such as collagen (COL4A5), chemokine (C–C motif) ligand 2, and desmocollin 2 (DSC2) were unique for OFC. It is intriguing that AFC and OFC expressed differently in functions which are not directly related to oxidative stress. The altered functions for AFC are metabolic pathways while for OFC are cell–cell interaction.

It is worthy to mention that cluster analysis recognized groups of genes with early response and late response. Early response genes include several genes associated with peroxi-

Table 3
Genes specifically up or downregulated in OFC

LLID	Symbol	AFC	OFC	FC	OFC/AFC	*P*-value[a]	Pathway[b]
10388	SYCP2	1.45	3.58	2.08	2.46	0.01835	Cytokinesis
4141	MARS	1.5	3.04	1.99	2.03	0.01486	**Methionyl-tRNA aminoacylation**
1824	DSC2	1.13	2.83	1.63	2.51	0.02016	**Homophilic cell adhesion**
51626	D2LIC	1.24	2.35	1.6	1.9	0.02581	
7221	TRPC2	1.14	2.26	1.5	1.99	0.04529	
80852	GRIP2	1.27	2.26	1.6	1.78	0.01233	
1287	COL4A5	1.34	2.25	1.65	1.67	0.00664	**Cell adhesion**
2796	GNRH1	1.14	2.19	1.48	1.92	0.01273	Cell–cell signaling
4295	MLN	1.07	2.16	1.42	2.01	0.00512	Cell–cell signaling
150160	CESK1	1.31	2.16	1.6	1.64	0.00123	**Protein folding**
94056	SYAP1	1.23	2.15	1.53	1.75	0.00264	
10420	TESK2	1.21	2.1	1.51	1.74	0.0101	Apoptosis
945	CD33	1.16	1.96	1.44	1.69	0.02362	Cell–cell signaling
3714	JAG2	0.8	1.93	1.14	2.41	0.02716	Regulation of cell proliferation
1258	CNGB1	0.92	0.55	0.75	0.6	0.05409	Potassium ion transport
53358	SHC3	0.98	0.55	0.78	0.57	0.0316	Intracellular signaling cascade
64116	SLC39A8	0.91	0.55	0.75	0.61	0.02339	Metal ion transport
23305	KIAA0837	1.02	0.53	0.78	0.51	0.03268	
3235	HOXD9	0.91	0.52	0.72	0.57	0.00566	Regulation of transcription DNA-dependent
4131	MAP1B	0.97	0.52	0.76	0.54	0.0348	
7355	SLC35A2	0.82	0.5	0.67	0.61	0.01838	Galactose metabolism
7386	UQCRFS1	0.8	0.49	0.66	0.61	0.00346	**Electron transport**
2731	GLDC	1.04	0.46	0.75	0.44	0.01506	**Glycine catabolism**
2950	GSTP1	0.9	0.46	0.68	0.51	0.03526	Metabolism
5360	PLTP	0.88	0.46	0.68	0.53	0.02491	Lipid metabolism
55644	OSGEP	1.12	0.43	0.77	0.39	0.03314	**Proteolysis and peptidolysis**
3117	HLA-DQA1	0.66	0.4	0.54	0.6	0.01553	Antigen processing exogenous antigen via MHC class II
1973	EIF4A1	1.3	0.39	0.81	0.3	0.04056	Regulation of translational initiation
6347	CCL2	0.66	0.39	0.53	0.58	0.00543	Inflammatory response
6628	SNRPB	0.61	0.37	0.5	0.61	0.00362	RNA splicing
6710	SPTB	0.63	0.26	0.44	0.41	0.00077	

[a]*P*-values depict results from *t*-test for all fold changes of OFC.
[b]Pathway is derived from GO-biological process. The plain text depicts representative pathway among several possible pathways. The bold text depicts unique pathway. The complete table is available on our website.

some (MVK, PXF, PXR1, and MLYCD) ande lyase activity (GAD1, IREB2, ODC1, PAICS, and MLYCD). Late response consist genes associated with glutathione biosynthesis (GGTLA1, GCLC, GCLM), acyl-CoA (MYO9B, PRKCD, PRKCG, PRKCH, KIAA0513), and more than 70 genes in protein metabolism.

3.3. Genes associated with oxidative stress were insufficient to distinguish AFC from OFC

To explore the possibility that genes associated with oxidative stress might be capable of distinguishing ac-LDL from ox-LDL foam cells, we performed a cluster analysis after selecting 95 genes listed in the category of oxidative stress (Fig. 2; genes are listed in Table 5, Supplementary Material). We observed no obvious pattern, suggesting that the expression pattern of genes associated with oxidative stress was insufficient to distinguish AFC from OFC.

3.4. Validation of expression by real-time RT-PCR

To validate common or unique expression of genes in AFC and OFC EGLN2, AKT1, PCTAIRE protein kinase 1 (PCTK1), and jagged 2 (JAG2) were selected for further analysis by real time RT-PCR (Fig. 3). ENGL2 is commonly upregulated and AKT1 is commonly downregulated both in AFC and OFC. PCTK1 is highly expressed in AFC and JAG2 is highly expressed in OFC. The time course-dependent expression in general agreed with microarray prediction.

3.5. Induction of IL1β suggested increased oxidative stress in cholesterol-loaded THP-1 cells

Interleukin 1 beta is a key enzyme for triggering cytokine response in cells; it is also a well-studied marker for OFC. IL1β was scored in the clusters that distinguished AFC from OFC.

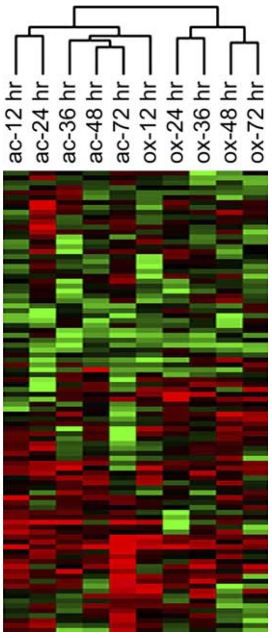

Fig. 2. Comparison of acetylated- and oxidized-LDL-loaded foam cells using the oxidative stress-specific gene expression ratios selected from the cDNA microarray.

We hypothesized that IL1β would exhibit a differential expression pattern between these two types of foam cells. To validate the transcriptional levels of interleukin 1 beta in the ac-LDL- and ox-LDL laden foam cells, we performed real-time RT-PCR of the total RNA extracted from macrophages administered with modified LDL and harvested the samples at various points of time (Fig. 4). The ox-LDL foam cells reached a high level of IL1β expression after 12 h; they maintained that level to the end. The internalization of ac-LDL by macrophages briefly induced a high level of IL1β expression after incubation for 12 h, but the transcriptional level dropped rapidly (to below fourfold after 24 h) and eventually returned to the normal level at the end of the time course.

The secretion of IL1β protein was obtained by ELISA (Fig. 5). IL1β was induced transiently in AFC while consistently maintained in OFC. The similar induction pattern of IL1β is consistent with the transcriptional results obtained by real-time RT-PCR.

3.6. Accumulation of superoxide in foam cells

Superoxide accumulation is a direct index of the oxidative stress present in foam cells [62]. We stained the foam cells with hydroethidine and then performed fluorescence imaging to quantify the fluorescence within their nuclei [47,48]. Fig. 6 presents the results of our time course experiment. For all of the foam cells, the fluorescence intensity rose rapidly, reached a plateau after 24 h, and then maintained a high level of intensity to the end. We noticed that the fluorescence levels of AFC dropped significantly after 36 h, but recovered and maintained a high level of fluorescence after 48 h. These hydroethidine staining experiments indicate that the steady state levels of superoxide in AFC and OFC remained high and that superoxide may contribute to the pathogenesis of disease progression.

3.7. Extracellular and intracellular oxidative modification

Cholesterol loading induced high levels of steady state superoxide that were indistinguishable in both AFC and OFC. Our results demonstrate that the internalization of cholesterol – without oxidative modification – by macrophages is sufficient to trigger cellular reactions leading to the generation of superoxide. We have reported previously that, upon internalization, ac-LDL generates the MDA-lysine epitope in foam cells [41]. It is plausible to suggest that cholesterol loading induces superoxide production, lipid peroxidation, and subsequent generation of MDA-modification to proteins. Lipid internalization, whether oxidative or non-oxidative, is a potent factor that increases the oxidative stress in macrophages.

Gene candidates that distinguish AFC from OFC may reveal the intricacies of these two entities. Functional annotation indicated deregulation for hormone activity, which we validated through the differential expression of IL1β in AFC and OFC. IL1β is the key enzyme in the inflammatory response. Although both ac-LDL and ox-LDL trigger inflammatory response in macrophages, OFC maintain high levels of IL1β expression, whereas AFC displayed only transient induction. The current study provided valuable lists for genes that are common or unique for AFC and OFC. Further study for the genes and function might prove beneficial to the pathogenesis of atherosclerosis.

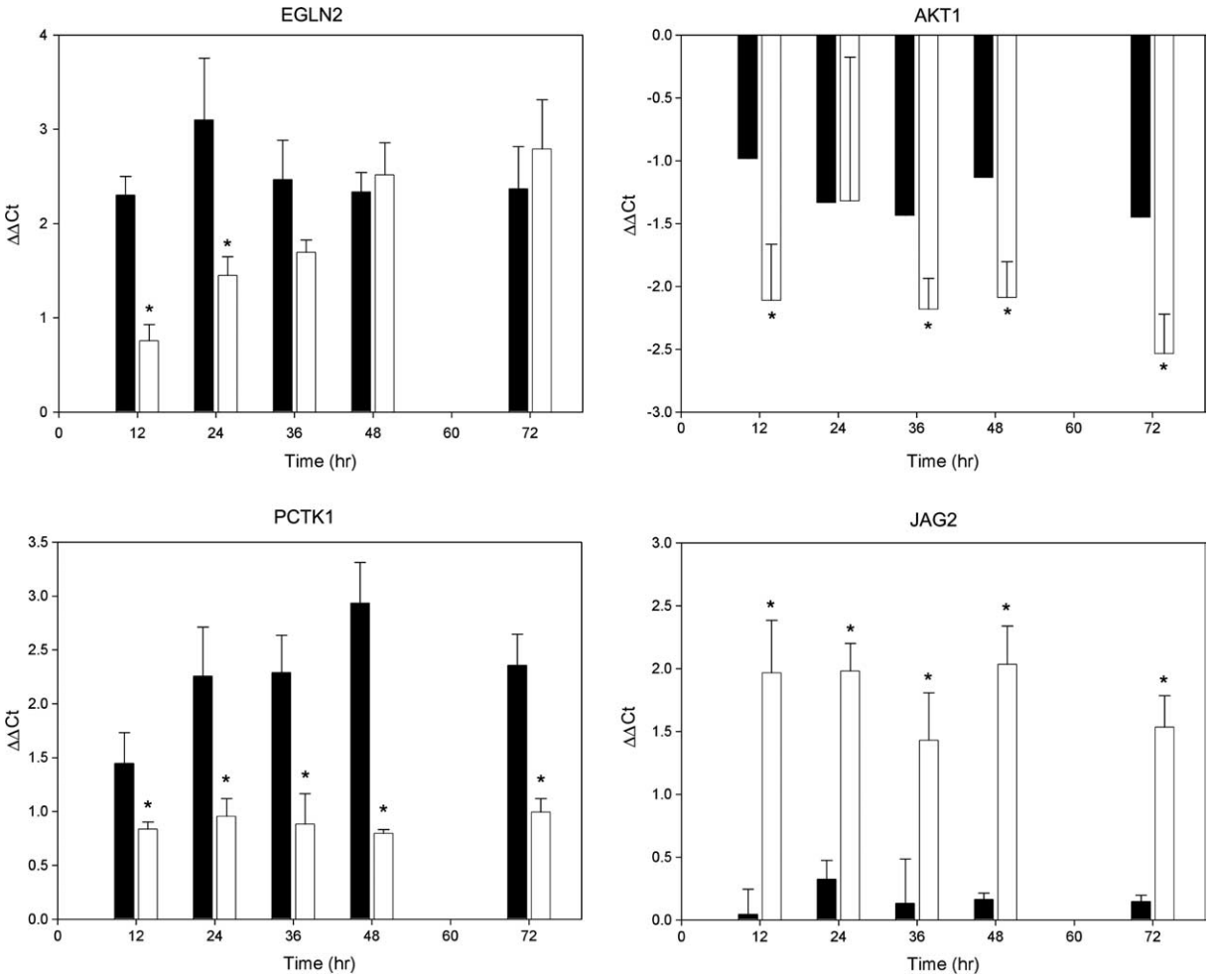

Fig. 3. Real-time RT-PCR showing time-course expression of ENGL2, AKT1, PCTK1, and JAG2 in AFC and OFC. Data is plotted based on $\Delta\Delta C_t$. The fold expression is equal to $2^{\Delta\Delta C_t}$. Each data point are the mean of three independent measurements and is expressed as means ± S.E.M. Asterisks depict significant differences between AFC and OFC. Solid bars, AFC; open bars, OFC.

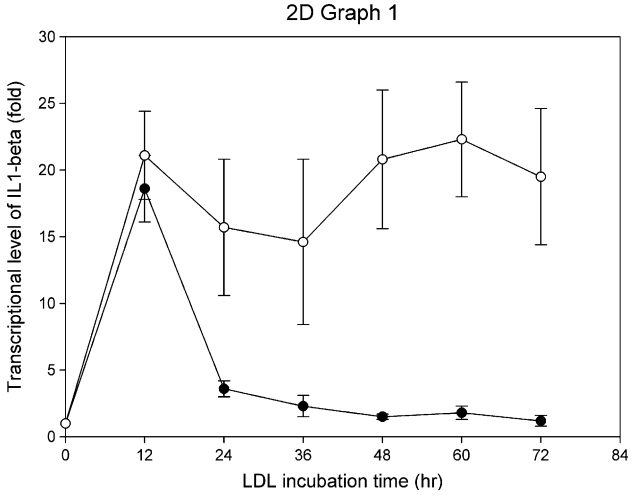

Fig. 4. Real-time RT-PCR and time-course experiments for the expression of interleukin 1beta in ac-LDL- and ox-LDL-laden foam cells. The fold expression is equal to $2^{\Delta\Delta C}$. Each data point are the mean of three independent measurements and is expressed as means ± S.E.M. Asterisks depict significant differences between AFC and OFC ($^{*}P < 0.05$; $^{**}P < 0.01$). Filled circle, AFC; open circle, OFC.

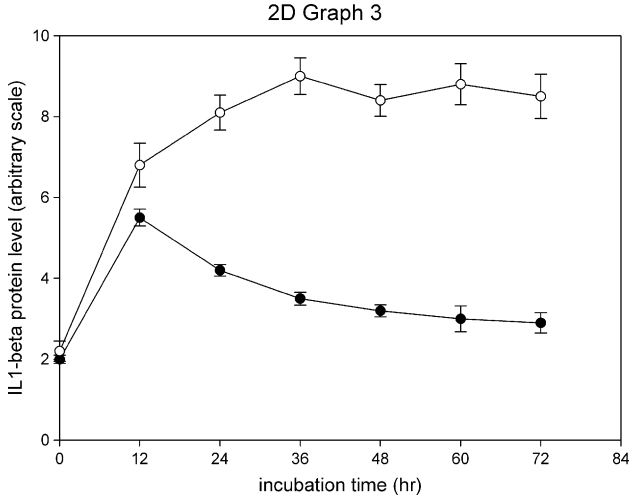

Fig. 5. IL1β protein level secreted by the cholesterol-loaded THP-1 cell ELISA was performed to the culture media of AFC and OFC in a time course experiment. Each data point are the mean of three independent measurements and is represented as the means ± S.E.M. Filled circle, AFC; open circle, OFC.

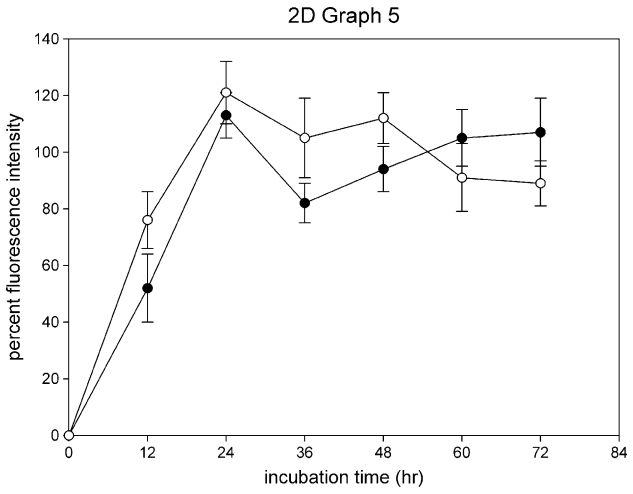

Fig. 6. Generation of free radicals following addition of ac-LDL and ox-LDL to macrophages. Fluorescence intensities are derived from image analysis; they are normalized against THP-1 cells and expressed as a percentage of the fluorescence intensities of OFC on day 3. Each data point are the mean of three independent measurements and is represented as the means ± S.E.M. Asterisks depict significant differences between AFC and OFC ($^{*}P < 0.05$; $^{**}P < 0.01$). Filled circle, AFC; open circle, OFC.

Acknowledgements: This work was supported in part by grants from the National Science Council, Taiwan (NSC90-2323-B-039-002, NSC91-2323-B-039-002, and NSC92-2314-B-039-022).

References

[1] Ross, R. (1993) The pathogenesis of atherosclerosis: a perspective for the 1990s. Nature 362, 801–809.
[2] Ross, R. (1986) The pathogenesis of atherosclerosis – an update. N. Engl. J. Med. 314, 488–500.
[3] Salonen, J.T. et al. (1992) Autoantibody against oxidised LDL and progression of carotid atherosclerosis [see comments]. Lancet 339, 883–887.
[4] Sasahara, M., Raines, E.W., Chait, A., Carew, T.E., Steinberg, D., Wahl, P.W. and Ross, R. (1994) Inhibition of hypercholesterolemia-induced atherosclerosis in the nonhuman primate by probucol. I. Is the extent of atherosclerosis related to resistance of LDL to oxidation? J. Clin. Invest. 94, 155–164.
[5] Alaupovic, P., Lee, D.M. and McConathy, W.J. (1972) Studies on the composition and structure of plasma lipoproteins. Distribution of lipoprotein families in major density classes of normal human plasma lipoproteins. Biochim. Biophys. Acta 260, 689–707.
[6] Jackson, R.L., Morrisett, J.D. and Gotto Jr., A.M. (1976) Lipoprotein structure and metabolism. Physiol. Rev. 56, 259–316.
[7] Brown, M.S. and Goldstein, J.L. (1990) Atherosclerosis. Scavenging for receptors [news]. Nature 343, 508–509.
[8] Freeman, M., Ashkenas, J., Rees, D.J., Kingsley, D.M., Copeland, N.G., Jenkins, N.A. and Krieger, M. (1990) An ancient, highly conserved family of cysteine-rich protein domains revealed by cloning type I and type II murine macrophage scavenger receptors. Proc. Natl. Acad. Sci. USA 87, 8810–8814.
[9] Sparrow, C.P., Parthasarathy, S. and Steinberg, D. (1989) A macrophage receptor that recognizes oxidized low density lipoprotein but not acetylated low density lipoprotein. J. Biol. Chem. 264, 2599–2604.
[10] Berliner, J.A., Navab, M., Fogelman, A.M., Frank, J.S., Demer, L.L., Edwards, P.A., Watson, A.D. and Lusis, A.J. (1995) Atherosclerosis: basic mechanisms. Oxidation, inflammation, and genetics. Circulation 91, 2488–2496.
[11] Steinberg, D., Parthasarathy, S. and Carew, T.E. (1988) In vivo inhibition of foam cell development by probucol in Watanabe rabbits. Am. J. Cardiol. 62, 6B–12B.
[12] Gerrity, R.G. and Naito, H.K. (1980) Alteration of endothelial cell surface morphology after experimental aortic coarctation. Artery 8, 267–274.
[13] Gerrity, R.G. (1981) The role of the monocyte in atherogenesis: II. Migration of foam cells from atherosclerotic lesions. Am. J. Pathol. 103, 191–200.
[14] Libby, P., Geng, Y.J., Aikawa, M., Schoenbeck, U., Mach, F., Clinton, S.K., Sukhova, G.K. and Lee, R.T. (1996) Macrophages and atherosclerotic plaque stability. Curr. Opin. Lipidol. 7, 330–335.
[15] Recchia, D., Abendschein, D.R., Saffitz, J.E. and Wickline, S.A. (1995) The biologic behavior of balloon hyperinflation-induced arterial lesions in hypercholesterolemic pigs depends on the presence of foam cells. Arterioscler. Thromb. Vasc. Biol. 15, 924–929.
[16] Rosenfeld, M.E. and Ross, R. (1990) Macrophage and smooth muscle cell proliferation in atherosclerotic lesions of WHHL and comparably hypercholesterolemic fat-fed rabbits. Arteriosclerosis 10, 680–687.
[17] Ku, G., Thomas, C.E., Akeson, A.L. and Jackson, R.L. (1992) Induction of interleukin 1 beta expression from human peripheral blood monocyte-derived macrophages by 9-hydroxyoctadecadienoic acid. J. Biol. Chem. 267, 14183–14188.
[18] Riessen, R., Isner, J.M., Blessing, E., Loushin, C., Nikol, S. and Wight, T.N. (1994) Regional differences in the distribution of the proteoglycans biglycan and decorin in the extracellular matrix of atherosclerotic and restenotic human coronary arteries. Am. J. Pathol. 144, 962–974.
[19] Guyton, J.R. and Klemp, K.F. (1989) The lipid-rich core region of human atherosclerotic fibrous plaques. Prevalence of small lipid droplets and vesicles by electron microscopy. Am. J. Pathol. 134, 705–717.
[20] Rosenfeld, M.E., Tsukada, T., Chait, A., Bierman, E.L., Gown, A.M. and Ross, R. (1987) Fatty streak expansion and maturation in Watanabe heritable hyperlipemic and comparably hypercholesterolemic fat-fed rabbits. Arteriosclerosis 7, 24–34.
[21] Reidy, M.A. (1994) Growth factors and arterial smooth muscle cell proliferation. Ann. NY Acad. Sci. 714, 225–230.
[22] Hagg, D. et al. (2005) Oxidized LDL induces a coordinated up-regulation of the glutathione and thioredoxin systems in human macrophages. Atherosclerosis 23, 23.
[23] Lutgens, E. et al. (2005) Gene profiling in atherosclerosis reveals a key role for small inducible cytokines: validation using a novel monocyte chemoattractant protein monoclonal antibody. Circulation 111, 3443–3452, (Epub 2005 Jun 20).
[24] Martinet, W., Schrijvers, D.M., De Meyer, G.R., Herman, A.G. and Kockx, M.M. (2003) Western array analysis of human atherosclerotic plaques: downregulation of apoptosis-linked gene 2. Cardiovasc. Res. 60, 259–267.
[25] Andersson, T., Borang, S., Larsson, M., Wirta, V., Wennborg, A., Lundeberg, J. and Odeberg, J. (2001) Novel candidate genes for atherosclerosis are identified by representational difference analysis-based transcript profiling of cholesterol-loaded macrophages. Pathobiology 69, 304–314.
[26] Andersson, T., Unneberg, P., Nilsson, P., Odeberg, J., Quackenbush, J. and Lundeberg, J. (2002) Monitoring of representational difference analysis subtraction procedures by global microarrays. Biotechniques 32, 1348–1350, 1352, 1354–6, 1358.
[27] Ohki, R., Yamamoto, K., Mano, H., Lee, R.T., Ikeda, U. and Shimada, K. (2002) Identification of mechanically induced genes in human monocytic cells by DNA microarrays. J. Hypertens. 20, 685–691.
[28] Shiffman, D. et al. (2000) Large scale gene expression analysis of cholesterol-loaded macrophages. J. Biol. Chem. 275, 37324–37332.
[29] Scholz, H. et al. (2005) Enhanced plasma levels of LIGHT in unstable angina: possible pathogenic role in foam cell formation and thrombosis. Circulation 112, 2121–2129, (Epub 2005 Sep 26).
[30] Svensson, P.A. et al. (2005) Major role of HSP70 as a paracrine inducer of cytokine production in human oxidized LDL treated macrophages. Atherosclerosis 30, 30.
[31] Takabe, W., Kanai, Y., Chairoungdua, A., Shibata, N., Toi, S., Kobayashi, M., Kodama, T. and Noguchi, N. (2004) Lysophosphatidylcholine enhances cytokine production of endothelial cells via induction of L-type amino acid transporter 1 and cell surface

antigen 4F2. Arterioscler. Thromb. Vasc. Biol. 24, 1640–1645, (Epub 2004 Jun 3).
[32] Brown, M.S., Basu, S.K., Falck, J.R., Ho, Y.K. and Goldstein, J.L. (1980) The scavenger cell pathway for lipoprotein degradation: specificity of the binding site that mediates the uptake of negatively-charged LDL by macrophages. J. Supramol. Struct. 13, 67–81.
[33] Brown, M.S. and Goldstein, J.L. (1983) Lipoprotein metabolism in the macrophage: implications for cholesterol deposition in atherosclerosis. Annu. Rev. Biochem. 52, 223–261.
[34] Goldstein, J.L., Ho, Y.K., Basu, S.K. and Brown, M.S. (1979) Binding site on macrophages that mediates uptake and degradation of acetylated low density lipoprotein, producing massive cholesterol deposition. Proc. Natl. Acad. Sci. USA 76, 333–337.
[35] Krieger, M., Acton, S., Ashkenas, J., Pearson, A., Penman, M. and Resnick, D. (1993) Molecular flypaper, host defense, and atherosclerosis. Structure, binding properties, and functions of macrophage scavenger receptors. J. Biol. Chem. 268, 4569–4572.
[36] Brown, M.S., Goldstein, J.L., Krieger, M., Ho, Y.K. and Anderson, R.G. (1979) Reversible accumulation of cholesteryl esters in macrophages incubated with acetylated lipoproteins. J. Cell Biol. 82, 597–613.
[37] Klein, R.L., Ascencao, J.L., Mironova, M., Huang, Y. and Lopes-Virella, M.F. (2001) Effect of inflammatory cytokines on the metabolism of low-density lipoproteins by human vascular endothelial cells. Metabolism 50, 99–106.
[38] Schena, M., Shalon, D., Davis, R.W. and Brown, P.O. (1995) Quantitative monitoring of gene expression patterns with a complementary DNA microarray [see comments]. Science 270, 467–470.
[39] Sparrow, C.P., Parthasarathy, S. and Steinberg, D. (1988) Enzymatic modification of low density lipoprotein by purified lipoxygenase plus phospholipase A2 mimics cell-mediated oxidative modification. J. Lipid Res. 29, 745–753.
[40] Mao, S.J., Rechtin, A.E., Krstenansky, J.L. and Jackson, R.L. (1990) Characterization of a monoclonal antibody specific to the amino terminus of the alpha-chain of human fibrin. Thromb. Haemost. 63, 445–448.
[41] Huang, G.S., Wang, Z.P., Wang, S.C., Sun, T.J., Chu, R. and Mao, S.J. (1999) Intracellular generation of MDA-LYS epitope in foam cells. Life Sci. 65, 285–296.
[42] Brazma, A. et al. (2001) Minimum information about a microarray experiment (MIAME)-toward standards for microarray data. Nat. Genet. 29, 365–371.
[43] Huang, G.S., Yang, S.M., Hong, M.Y., Yang, P.C. and Liu, Y.C. (2000) Differential gene expression of livers from ApoE deficient mice. Life Sci. 68, 19–28.
[44] Cleveland, W.S. (1979) Robust locally weighted regression and smoothing scatterplots. J. Am. Stat. Assoc. 74, 829–836.
[45] Tusher, V.G., Tibshirani, R. and Chu, G. (2001) Significance analysis of microarrays applied to the ionizing radiation response. Proc. Natl. Acad. Sci. USA 98, 5116–5121, (Epub 2001 Apr 17).
[46] Morrison, T.B., Weis, J.J. and Wittwer, C.T. (1998) Quantification of low-copy transcripts by continuous SYBR Green I monitoring during amplification. Biotechniques 24, 954–958, 960, 962.
[47] Suzuki, H., Swei, A., Zweifach, B.W. and Schmid-Schonbein, G.W. (1995) In vivo evidence for microvascular oxidative stress in spontaneously hypertensive rats. Hydroethidine microfluorography. Hypertension 25, 1083–1089.
[48] Bindokas, V.P., Jordan, J., Lee, C.C. and Miller, R.J. (1996) Superoxide production in rat hippocampal neurons: selective imaging with hydroethidine. J. Neurosci. 16, 1324–1336.
[49] Lacoviello, L. et al. (2005) Polymorphisms of the interleukin-1beta gene affect the risk of myocardial infarction and ischemic stroke at young age and the response of mononuclear cells to stimulation in vitro. Arterioscler. Thromb. Vasc. Biol. 25, 222–227, (Epub 2004 Nov 11).
[50] Woodside, K.J., Hernandez, A., Smith, F.W., Xue, X.Y., Hu, M., Daller, J.A. and Hunter, G.C. (2003) Differential gene expression in primary and recurrent carotid stenosis. Biochem. Biophys. Res. Commun. 302, 509–514.
[51] Wilson, S.H., Herrmann, J., Lerman, L.O., Holmes Jr., D.R., Napoli, C., Ritman, E.L. and Lerman, A. (2002) Simvastatin preserves the structure of coronary adventitial vasa vasorum in experimental hypercholesterolemia independent of lipid lowering. Circulation 105, 415–418.
[52] Zhu, X.Y. et al. (2004) Antioxidant intervention attenuates myocardial neovascularization in hypercholesterolemia. Circulation 109, 2109–2115, (Epub 2004 Mar 29).
[53] Johnson, W.J., Phillips, M.C. and Rothblat, G.H. (1997) Lipoproteins and cellular cholesterol homeostasis. Subcell Biochem. 28, 235–276.
[54] Billheimer, J.T. and Reinhart, M.P. (1990) Intracellular trafficking of sterols. Subcell Biochem. 16, 301–331.
[55] Babal, P. and Pechanova, O. (1992) Activity of ATPase and 5′ nucleotidase in endothelium of human atherosclerotic aortas. Cor. Vasa. 34, 238–245.
[56] Gillies, P. and Robinson, C. (1988) Decreased plasma membrane fluidity in the development of atherosclerosis in cholesterol-fed rabbits. Atherosclerosis 70, 161–164.
[57] Li, A.C. et al. (2004) Differential inhibition of macrophage foam-cell formation and atherosclerosis in mice by PPARalpha, beta/delta, and gamma. J. Clin. Invest. 114, 1564–1576.
[58] Tham, D.M., Wang, Y.X. and Rutledge, J.C. (2003) Modulation of vascular inflammation by PPARs. Drug News Perspect. 16, 109–116.
[59] Silverstein, R.L. and Nachman, R.L. (1987) Thrombospondin binds to monocytes–macrophages and mediates platelet–monocyte adhesion. J. Clin. Invest. 79, 867–874.
[60] Strickland, D.K., Kounnas, M.Z. and Argraves, W.S. (1995) LDL receptor-related protein: a multiligand receptor for lipoprotein and proteinase catabolism. Faseb J. 9, 890–898.
[61] Fuhrman, B., Oiknine, J. and Aviram, M. (1994) Iron induces lipid peroxidation in cultured macrophages, increases their ability to oxidatively modify LDL, and affects their secretory properties. Atherosclerosis 111, 65–78.
[62] Iuliano, L. (2001) The oxidant stress hypothesis of atherogenesis. Lipids 36, S41–S44.